Boeing 737 Six DOF Dynamics

ECE 242: Nonlinear Dynamic Systems

Linzhe (Jeremy) Wang

Winter 2023

Contents

List of Figures

List of Tables

1 Introduction

As the motivation for developing advanced aircraft systems continues to grow, a significant demand exists for high-fidelity dynamics simulation platforms to accelerate the design cycles and lower the project cost. Current popular topics in the aerospace industry include but are not limited to Unmanned Aerial Systems (UAS) and Urban Air Mobility (UAM), which all require extensive simulation data to ensure the safe deployment of prototype flight tests. The initial step of implementing aircraft simulations is to build a dynamic model to incorporate aerodynamics from wind tunnel tests or computational methods. Nonetheless, aircraft is extraordinarily complex and highly nonlinear, in which the system may have finite escape time, non-unique solutions, and periodic orbits. Hence, it is critical to study and understand the aircraft system's nonlinear behaviors before developing simulations.

The project aims to investigate the nonlinear effects of the aircraft using a six-DOF dynamic model. The system consists of nine coupled nonlinear differential equations describing the aircraft's orientation and exerted forces. The nine states evolve with time and contain periodic cycles, stability issues, and solutions that are not defined for all time, making the model a nonlinear dynamical system.

1.1 The Rigid Nonlinear Aircraft Model

Consider a complete rigid-body aircraft; the moments and aerodynamic forces applied on an aircraft are caused by relative motion with respect to the air and aircraft orientation to free-stream air. Thus, the dynamical system is constructed via force, kinematic, and moment equations [1]. Equation 1 describes the aircraft's velocity with respect to the X-Y-Z axes. Equation 2 contains the Euler angle rates to identify the orientation of an aircraft. Equation 3 provides the roll, pitch, and yaw rate measurements with respect to the X-Y-Z axes. Combining nine equations provide the rigid nonlinear aircraft model.

Force Equations:

$$\begin{aligned} \dot{U} &= RV - QW - g_0' \sin\theta + \frac{F_x}{m} \\ \dot{V} &= -RV + PW + g_0' \sin\phi\cos\theta + \frac{F_y}{m} \\ \dot{W} &= QU - PV + g_0' \cos\phi\cos\theta + \frac{F_z}{m} \end{aligned} \tag{1}$$

Kinematic Equations:

$$\begin{aligned} \dot{\phi} &= P + \tan\theta(Q\sin\phi + R\cos\phi) \\ \dot{\theta} &= Q\cos\phi - R\sin\phi \\ \dot{\psi} &= \frac{Q\sin\phi}{\cos\theta} + \frac{R\cos\phi}{\cos\theta} \end{aligned} \tag{2}$$

Moment Equations:

$$\begin{aligned}\dot{P} &= (c_1 R + c_2 P)Q + c_3 \bar{L} + c_4 N \\ \dot{Q} &= c_5 PR - c_6(P^2 - R^2) + c_7 M \\ \dot{R} &= (c_8 P - c_2 R)Q + c_4 \bar{L} + c_9 N\end{aligned} \tag{3}$$

The c_i coefficients are derived from the inertia matrix (J) of the rigid body under the plane-of-symmetry assumption:

$$J = \begin{bmatrix} J_x & 0 & -J_{xz} \\ 0 & J_y & 0 \\ -J_{xz} & 0 & J_z \end{bmatrix}, \quad \Gamma = J_x J_z - J_{xz}^2 \tag{4}$$

$$\begin{aligned} \Gamma c_1 &= (J_y - J_z)J_z - J_{xz}^2, & \Gamma c_2 &= (J_x - J_y + J_z)J_x z \\ \Gamma c_3 &= J_z, & \Gamma c_4 &= J_{xz} \\ c_5 &= \frac{J_z - J_x}{J_y}, & c_6 &= \frac{J_{xz}}{J_y} \\ c_7 &= \frac{1}{J_y}, & \Gamma c_8 &= J_x(J_x - J_y) + J_{xz}^2 \\ \Gamma c_9 &= J_x \end{aligned} \tag{5}$$

1.2 Force and Moment Coefficients

The forces and moments acting on the aircraft are defined via dimensionless aerodynamic parameters such as lift and drag coefficients. These coefficients are collected using wind tunnel tests and computational fluid dynamics (CFD) data based on a specific physical model. Different aircraft geometries can have various performances and flight envelopes. Thus, the current project utilizes aerodynamic coefficients based on a Boeing 737 airplane obtained from Group for Aeronautical Research and Technology in Europe (GARTEUR) [2].

Aerodynamic Forces and Moments:

$$\begin{aligned} drag, \quad & D = \bar{q}SC_D \\ lift, \quad & L = \bar{q}SC_L \\ sideforce, \quad & Y = \bar{q}SC_Y \\ rolling\ moment, \quad & \bar{L} = \bar{q}SbC_l \\ pitching\ moment, \quad & M = \bar{q}S\bar{c}C_M \\ yawing\ moment, \quad & N = \bar{q}SbC_N \end{aligned} \tag{6}$$

$$\begin{aligned} free\ stream\ dynamic\ pressure &= \bar{q} \\ wing\ reference\ area &= S \\ wing\ span &= b \\ wing\ mean\ geometric\ chord &= \bar{c} \end{aligned}$$

Aerodynamic Forces in Body-Axes:

$$
\begin{aligned}
F_x &= L\sin\alpha - D\cos\alpha\cos\beta - Y\cos\alpha\sin\beta \\
F_y &= -D\sin\beta + Y\cos\beta \\
F_z &= -L\cos\alpha - D\sin\alpha\cos\beta - Y\sin\alpha\sin\beta
\end{aligned}
\tag{7}
$$

$$
\begin{aligned}
\alpha &= angle\,of\,attack \\
\beta &= angle\,of\,sideslip
\end{aligned}
$$

1.3 Applications

Due to the high cost of building prototypes and conducting real-world flight tests, the ability to develop high-fidelity dynamic models becomes essential during the design cycles. Many aerospace corporations, such as Textron Aviation, rely on simulations to validate the flight envelope in the preliminary design phase. Additionally, the nonlinear model introduced in Sec. 1.1 works for all types of rigid-body aircraft. Since the modeling process is often iterative, more complexities are applied to the dynamic models, but the nonlinear model serves as the critical first step in development.

2 Stability Analysis

2.1 Description of the Dynamical System

A dynamical system can be precisely described using the notation $\Sigma = (T, X, \Phi, D_\Phi)$, where T is a time-domain, $T \subseteq \mathbb{R}$, X is a state space, $D_\Phi \subset T \times T \times X$, and $\Phi : D_\Phi \mapsto X$ such that $\Phi(t, t_0, x_0) = x_0$. Following the notation, the rigid nonlinear aircraft model is defined in Eq. 8-9, representing a state-space model in terms of nine state variables. The system is described by a set of ordinary differential equations, where the time derivative of the state vector $\mathbf{x}$ is given by the vector of functions $\dot{\mathbf{x}} = [\dot{U}, \dot{V}, \dot{W}, \dot{\phi}, \dot{\theta}, \dot{\psi}, \dot{P}, \dot{Q}, \dot{R}]^T$. The system can be written in matrix form as $\dot{x} = f(x,t) + g(x,t)u$, where $f(x)$ is a vector function of the state variables x, and $g(x,t)$ is a vector function of external inputs (forces and moments).

The state space, the set of all possible and known states of a system, can be defined as $X = \mathbb{R}^9$, and $T = (0, \infty)$. Then, $D_\Phi = (0,\infty) \times (0,\infty) \times \mathbb{R}^9$, and $\Phi : \mathbb{R}^9 \mapsto \mathbb{R}^9$. The condition of $\Phi(t, t_0, x_0) = x_0$ is satisfied and proved via simulations in Sec. 2.2. Additionally, this is a continuous-time dynamical system because the time-domain T is defined as continuous.

A forward trajectory is defined as the mapping $t \mapsto \Phi(t, t_0, x_0)$, where $t \in T_{(t_0,x_0)} \cap T_{\geqslant} t_0$. Hence, the trajectory of this system is oscillatory, which is plotted in Sec. 2.2. Throughout the project, simulations are utilized to demonstrate the results of various nonlinear behaviors of the dynamical system. Thus, a Simulink model is developed to solve the system and produce data, as shown in Fig. 1. The Simulink model is designed with actuators, aircraft dynamics, geodetic position, and atmosphere models to provide a high-fidelity simulation environment.

$$\Phi(t, t_0, x_0) = \dot{x} = f(x,t) + g(x,t)u \tag{8}$$

$$\Phi(t, t_0, x_0) = \begin{bmatrix} \dot{x_1} \\ \dot{x_2} \\ \dot{x_3} \\ \dot{x_4} \\ \dot{x_5} \\ \dot{x_6} \\ \dot{x_7} \\ \dot{x_8} \\ \dot{x_9} \end{bmatrix} = \begin{bmatrix} \dot{U} \\ \dot{V} \\ \dot{W} \\ \dot{\phi} \\ \dot{\theta} \\ \dot{\psi} \\ \dot{P} \\ \dot{Q} \\ \dot{R} \end{bmatrix} = \begin{bmatrix} x_9 x_2 - x_8 x_3 - g_0' \sin x_5 \\ -x_9 x_2 + x_7 x_3 + g_0' \sin x_4 \cos x_5 \\ x_8 x_1 - x_7 x_2 + g_0' \cos x_4 \cos x_5 \\ x_7 + \tan x_5 (x_8 \sin x_4 + x_9 \cos x_4) \\ x_8 \cos x_4 - x_9 \sin x_4 \\ \frac{x_8 \sin x_4}{\cos x_5} + \frac{x_9 \cos x_4}{\cos x_5} \\ (c_1 x_9 + c_2 x_7) x_8 \\ c_5 x_7 x_9 - c_6 (x_7^2 - x_9^2) \\ (c_8 x_7 - c_2 x_9) x_8 \end{bmatrix} + \begin{bmatrix} \frac{F_x}{m} \\ \frac{F_y}{m} \\ \frac{F_z}{m} \\ 0 \\ 0 \\ 0 \\ c_3 \bar{L} + c_4 N \\ c_7 M \\ c_4 \bar{L} + c_9 N \end{bmatrix} u \tag{9}$$

2.2 Periodic Orbits

A forward fixed point from t_0 to t for Σ is a point x^* such that $\phi(t, t_0, x^*) = x^*$ for all $t \in T_{(t_0,x^*)}$. Consider the dynamical system described in Sec. 2.1, where the states are defined as $x = [U, V, W, \phi, \theta, \psi, P, Q, R]$. Now, define a set of initial conditions such that

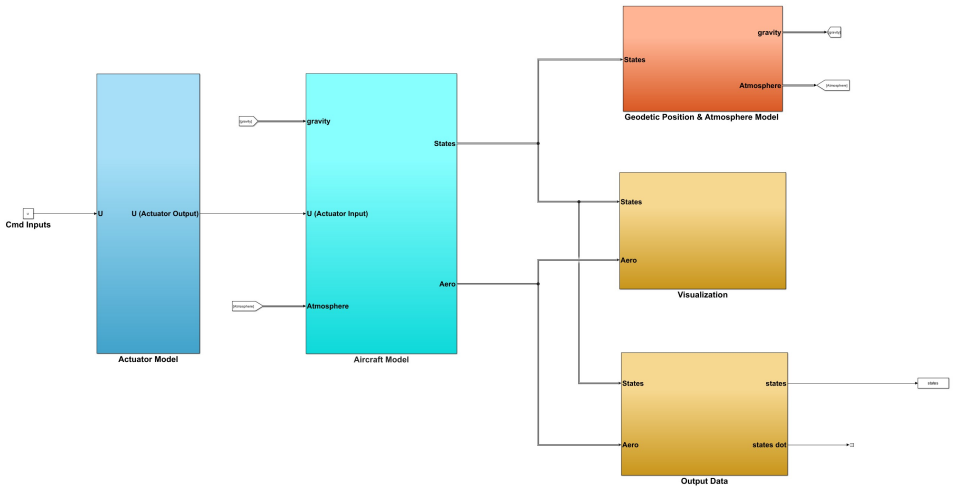

Figure 1: Rigid nonlinear aircraft simulink model

$x_0 = [80, 0, 0, 0, 0, 0, 0, 0, 0]$ to solve the dynamical system. Then, a set of fixed point x^* can be found numerically using a sequential quadratic programming algorithm, where the computed x^* is shown in Eq. 10. The fixed point can be verified by utilizing simulations, as shown in Fig. 2-4. It can be observed that the dynamical system is converged to the fixed point value, which satisfies the definition of $\phi(1000s, 0s, x^*) = x^*$.

$$x^* = [80.0000, 0.0000, 3.2235, 0.0000, -0.0844, 0.0000, 0.0000, 0.0000, 0.0000] \quad (10)$$

The periodic orbit behaviors are also expected to see in the dynamical system, where the nearby solutions are converged to the periodic orbit. To illustrate, two sets of initial states are constructed to solve the system, as shown in Tab. 1. Each initial condition is varied by increasing the velocity in x direction. Simulation results are presented in Fig. 5-7, and it can be noted that all differential equations are converged to a periodic orbit with various initial conditions. In fact, this phenomenon is anticipated to occur in nonlinear systems for all dimensions above one.

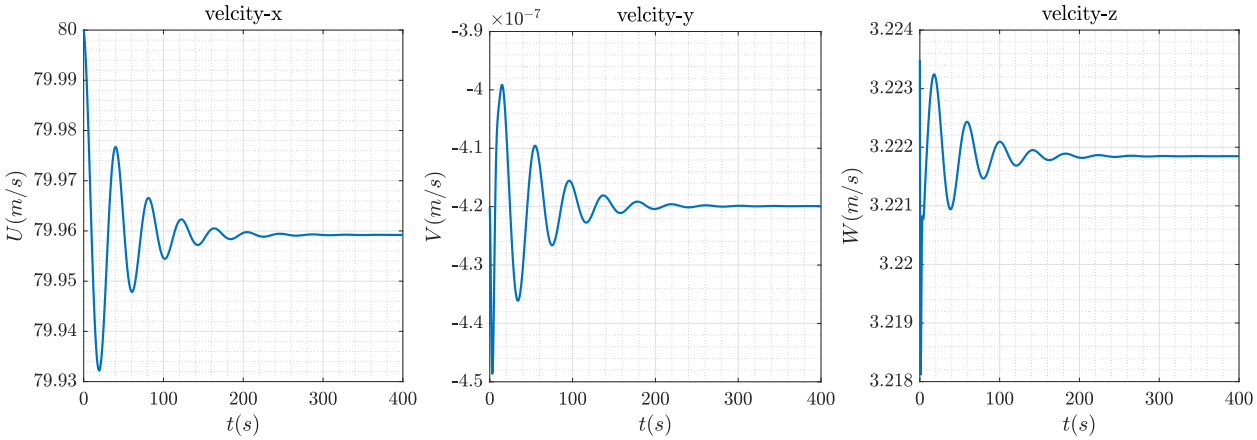

Figure 2: Fixed point verification for force equations

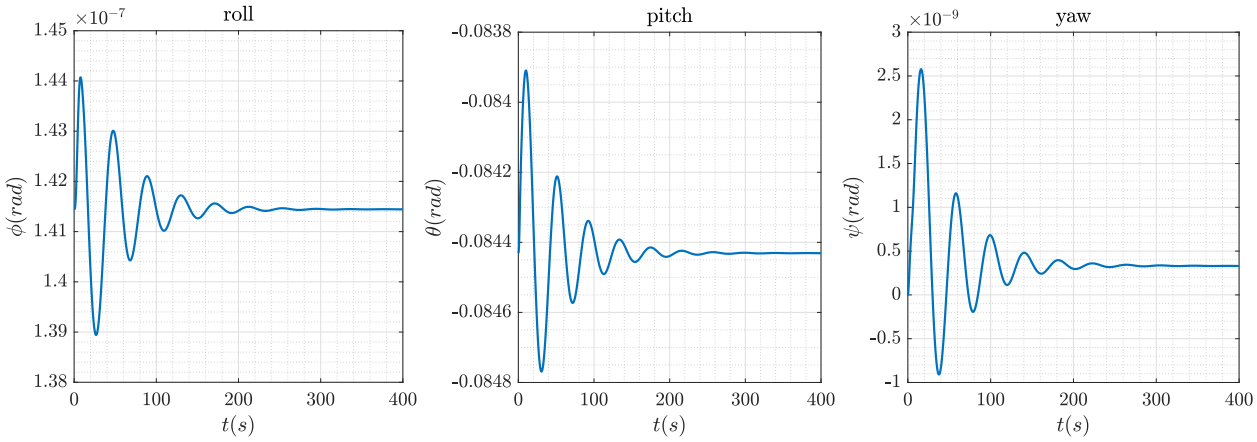

Figure 3: Fixed point verification for kinematic equations

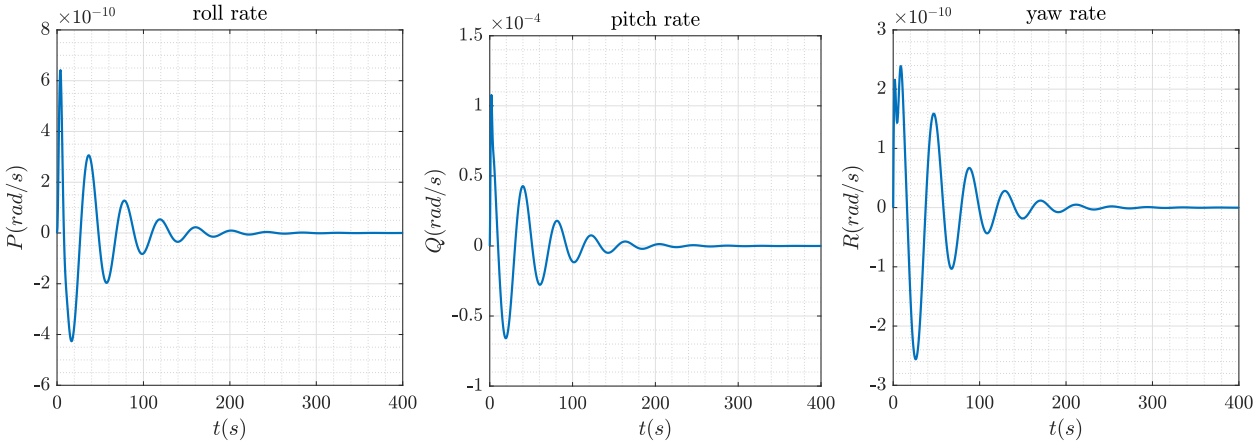

Figure 4: Fixed point verification for moment equations

Table 1: Initial states for periodic orbit simulations

	x
initial state 1	[80.0000,0.0000,3.2235,0.0000,-0.0844,0.0000,0.0000,0.0000,0.0000]
initial state 2	[82.0000,0.0000,3.2235,0.0000,-0.0844,0.0000,0.0000,0.0000,0.0000]

2.3 Existence and Uniqueness

The existence and uniqueness of a nonlinear dynamical system can be proved using Picard iterations and applying the Contraction Mapping Principle. Consider Picard's method of approximation defined in Eq. 11, which is computed on a bounded interval. Then, if a fixed-point x^* of the Picard operator exists, the solution satisfies the initial value problem. Therefore, proving existence and uniqueness of solutions is equivalent to showing that the Picard operator has a unique fixed point, as shown in Eq. 12.

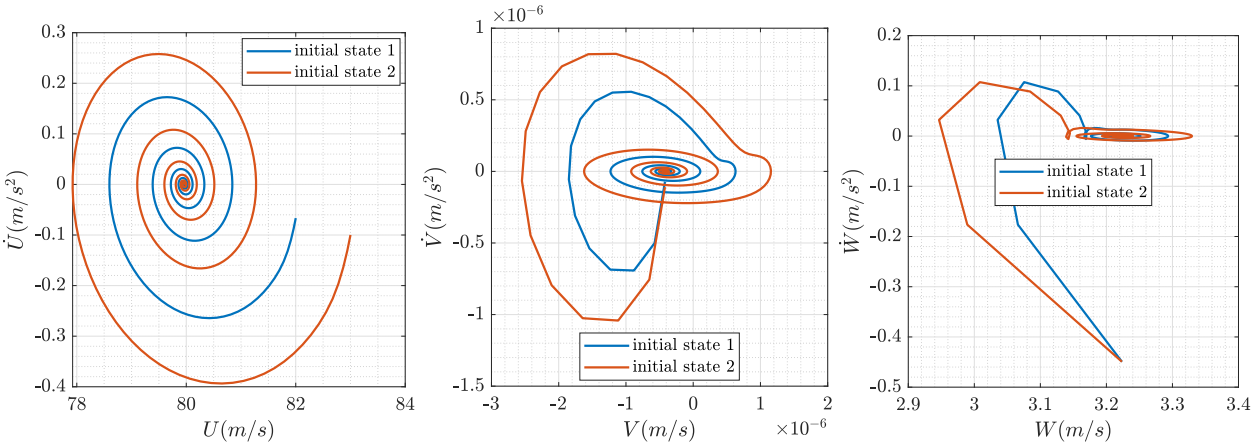

Figure 5: Periodic orbits for force equations

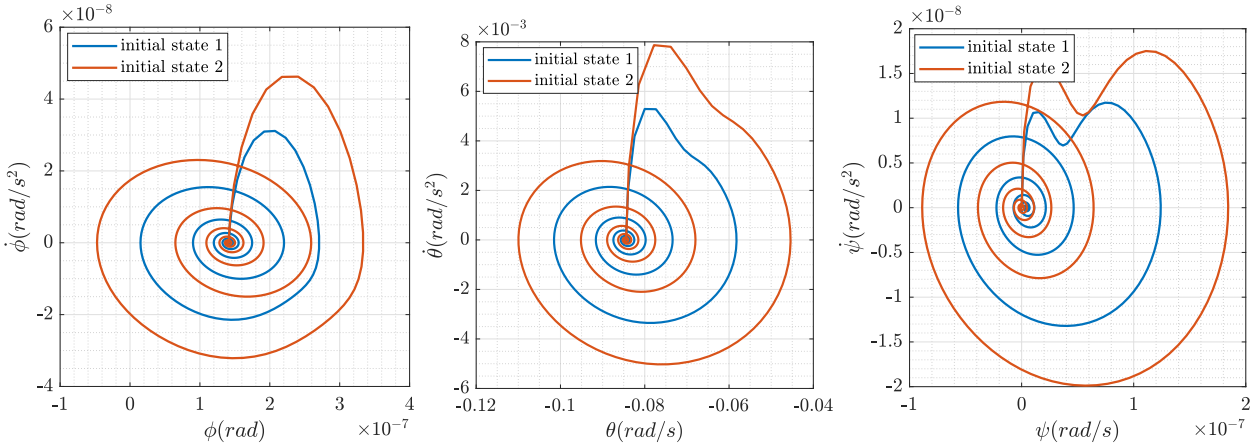

Figure 6: Periodic orbits for kinematic equations

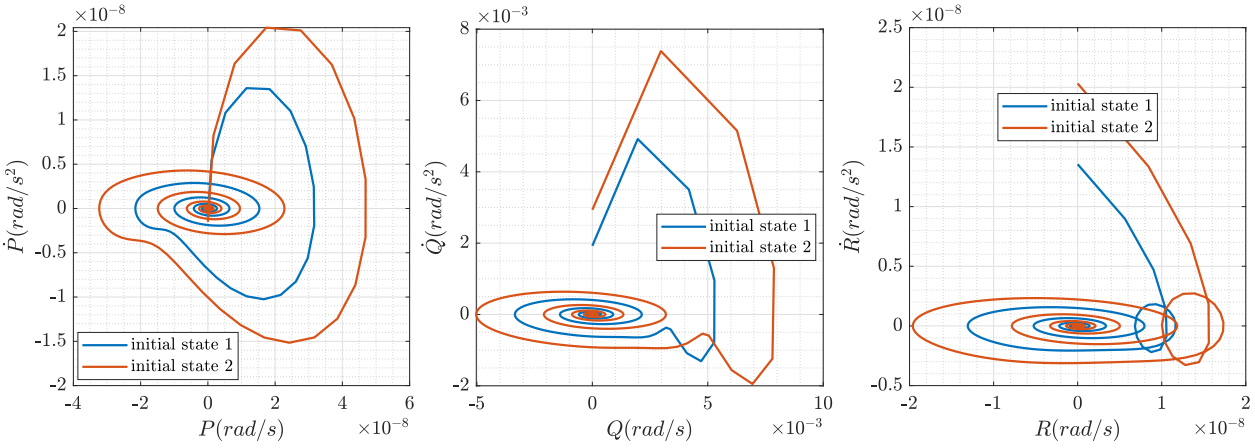

Figure 7: Periodic orbits for moment equations

$$
\begin{aligned}
z_0(t) &= x_0 \\
z_{n+1}(t) &= x_0 + \int_{t_0}^{t} f(z_n(\tau))\, d\tau, \quad n \in \mathbb{N}
\end{aligned}
\tag{11}
$$

$$
x^* = P(x^*) \quad \Longrightarrow \quad x^*(t) = P(x^*)(t) = x_0 + \int_{t_0}^{t} f(x^*(s))\, ds \tag{12}
$$

Now, apply the Picard iterations to the dynamical system defined in Sec. 2.1. Consider only the x-velocity equation $\dot{x_1} = x_9x_2 - x_8x_3 - g_0' \sin x_5 + \frac{F_x}{m}$, a locally Lipshitz continuous function, and $x_1(0) = x_{1,0}$. For simplicity, set $(x_9x_2 - x_8x_3 - g_0' \sin x_5 + \frac{F_x}{m})(t) = \alpha(t)$ since these terms are not a function of x_1. The analytical solution is provided in Eq. 13, which cannot be evaluated explicitly because terms such as x_9 and x_2 depending on time and other states. Due to the high complexities of the dynamical system, the closed-form solution of the system cannot be obtained. Thus, it is challenging to verify if the Picard iteration solution is equivalent to the original solution given x^* such that $x^*(t) = P(x^*)(t) = x_0 + \int_{t_0}^{t} f(x^*(s))\, ds$.

$$
\begin{aligned}
z_0(t) &= x_1(0) \\
z_1(t) &= x_1(0) + \int_0^t \alpha(t)x_1(0)\, ds = (1 + \alpha(t)t)x_1(0) \\
z_2(t) &= x_1(0) + \int_0^t \alpha(t)(1 + \alpha(t)s)x_1(0)\, ds = (1 + \alpha(t)t + \frac{1}{2}\alpha(t)^2t^2)x_1(0) \\
z_3(t) &= x_1(0) + \int_0^t \alpha(t)(1 + \alpha(t)s + \frac{1}{2}\alpha(t)^2t^2)x_1(0)\, ds = (1 + \alpha(t)t + \frac{1}{2}\alpha(t)^2t^2 + \frac{1}{3!}\alpha(t)^3t^3)x_1(0), \quad ... \\
z_n(t) &= \sum_{k=0}^{n} \frac{\alpha(t)^k t^k}{k!} x_1(0) \\
z_n(t) &= \sum_{k=0}^{n} \frac{(x_9x_2 - x_8x_3 - g_0' \sin x_5 + \frac{F_x}{m})(t)^k t^k}{k!} x_1(0)
\end{aligned}
\tag{13}
$$

Section 2.2 suggests that the system solutions exist. Then, another way to verify the uniqueness of the solutions is to check if $\frac{df}{dx_1}$ is continuous near (t_0, x^*). In other words, since the Picard-Lindelof theorem requires the function to satisfy Lipschitz continuity, and differentiability guarantees continuity. Therefore, a unique solution must be differentiable. Equation 14 suggests that the function is continuous; thus, the solution to $\dot{x_1}$ is unique. Similarly, the technique can be applied to the entire system Σ, as shown in Eq. 15-22. Thus, it is safe to assume that the system solutions are unique and that trajectories exist locally.

$$
\begin{aligned}
\frac{df}{dx_1}\Big|_{(t_0,x^*)} &= \frac{d(x_9x_2 - x_8x_3 - g_0' \sin x_5 + \frac{F_x}{m})}{dx_1} \\
\frac{df}{dx_1}\Big|_{(0,x^*)} &= 0 \quad \Longrightarrow \quad \textit{continuous}
\end{aligned}
\tag{14}
$$

$$\frac{df}{dx_2}\Big|_{(t_0,x^*)} = \frac{d(-x_9x_2 + x_7x_3 + g_0' \sin x_4 \cos x_5 + \frac{F_y}{m})}{dx_2}$$
$$\frac{df}{dx_2}\Big|_{(t_0,x^*)} = -x_9, \quad x_9 = 0 \tag{15}$$
$$\frac{df}{dx_2}\Big|_{(0,x^*)} = 0 \quad \Longrightarrow \quad continuous$$

$$\frac{df}{dx_3}\Big|_{(t_0,x^*)} = \frac{d(x_8x_1 - x_7x_2 + g_0' \cos x_4 \cos x_5 + \frac{F_z}{m})}{dx_3} \tag{16}$$
$$\frac{df}{dx_3}\Big|_{(0,x^*)} = 0 \quad \Longrightarrow \quad continuous$$

$$\frac{df}{dx_4}\Big|_{(t_0,x^*)} = \frac{d(x_7 + \tan x_5(x_8 \sin x_4 + x_9 \cos x_4))}{dx_4}$$
$$\frac{df}{dx_4}\Big|_{(t_0,x^*)} = \tan x_5 x_8 \cos x_4 - x_9 \sin x_4, \quad x_4 = x_8 = 0 \tag{17}$$
$$\frac{df}{dx_4}\Big|_{(0,x^*)} = 0 \quad \Longrightarrow \quad continuous$$

$$\frac{df}{dx_5}\Big|_{(t_0,x^*)} = \frac{d(x_8 \cos x_4 - x_9 \sin x_4))}{dx_5} \tag{18}$$
$$\frac{df}{dx_5}\Big|_{(0,x^*)} = 0 \quad \Longrightarrow \quad continuous$$

$$\frac{df}{dx_6}\Big|_{(t_0,x^*)} = \frac{d(\frac{x_8 \sin x_4}{\cos x_5} + \frac{x_9 \cos x_4}{\cos x_5}))}{dx_6} \tag{19}$$
$$\frac{df}{dx_6}\Big|_{(0,x^*)} = 0 \quad \Longrightarrow \quad continuous$$

$$\frac{df}{dx_7}\Big|_{(t_0,x^*)} = \frac{d((c_1x_9 + c_2x_7)x_8 + c_3\bar{L} + c_4N)}{dx_7}$$
$$\frac{df}{dx_7}\Big|_{(t_0,x^*)} = c_2x_8, \quad x_8 = 0 \tag{20}$$
$$\frac{df}{dx_7}\Big|_{(0,x^*)} = 0 \quad \Longrightarrow \quad continuous$$

$$\frac{df}{dx_8}\Big|_{(t_0,x^*)} = \frac{d((c_5x_7x_9 - c_6(x_7^2 - x_9^2) + c_7M)}{dx_8} \tag{21}$$
$$\frac{df}{dx_8}\Big|_{(0,x^*)} = 0 \quad \Longrightarrow \quad continuous$$

$$\frac{df}{dx_9}\Big|_{(t_0,x^*)} = \frac{d(((c_8x_7 - c_2x_9)x_8 + c_4\bar{L} + c_9N)}{dx_9}$$
$$\frac{df}{dx_9}\Big|_{(0,x^*)} = -c_2x_8, \quad x_8 = 0 \tag{22}$$
$$\frac{df}{dx_9}\Big|_{(0,x^*)} = 0 \quad \Longrightarrow \quad continuous$$

2.4 Regularity

Consider a dynamical system:

$$\begin{aligned} \dot{x}(t) &= f(t, x(t)), \quad T = [a, b] \\ x(t_0) &= x_0 \end{aligned} \tag{23}$$

Suppose that f is in c^k, and there exists a neighborhood of x_0 and a sub interval of time around t_0 such that the solution (flow ϕ^f) is in c^k. Then, apply the definition to the nonlinear aircraft dynamical system described in Sec. 2.1. The time domain can be defined as $T = [20, 50]$ because the system is not differentiable for all time. To illustrate the regularity definition, simulations are developed such that the initial state one can make the system satisfy c^k, and the neighborhood of initial state one is generated, making the system satisfy c^k regularity. Simulation results are shown in Fig. 8-10, and initial conditions applied to the system are shown in Tab. 2. Under the bounded time interval, the plots appear to have smooth curves without any sudden slope changes and are likely to be differentiable at those points. Hence, the dynamical system has some degree of c^k regularity, which is not affected by the initial conditions.

Table 2: Initial states for regularity simulations

	x_0
initial state 1	[80.0,0.0,0.0,0.0,0.0,0.0,0.0,0.0,0.0,0.0,0.0,0.0]
initial state 2	[91.0,0.0,0.0,0.0,0.0,0.0,0.0,0.0,0.0,0.0,0.0,0.0]
initial state 3	[93.0,0.0,0.0,0.0,0.0,0.0,0.0,0.0,0.0,0.0,0.0,0.0]

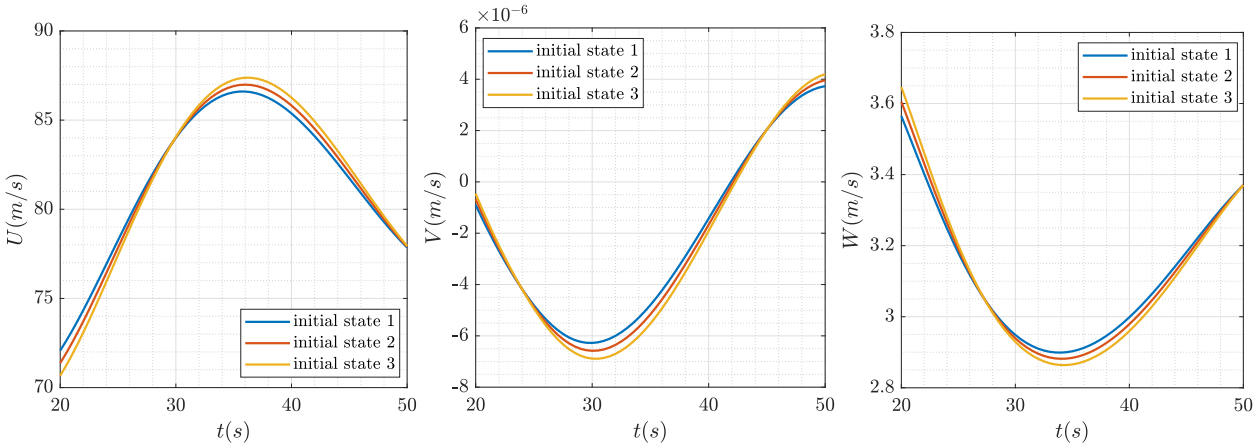

Figure 8: Regularity verification for force equations

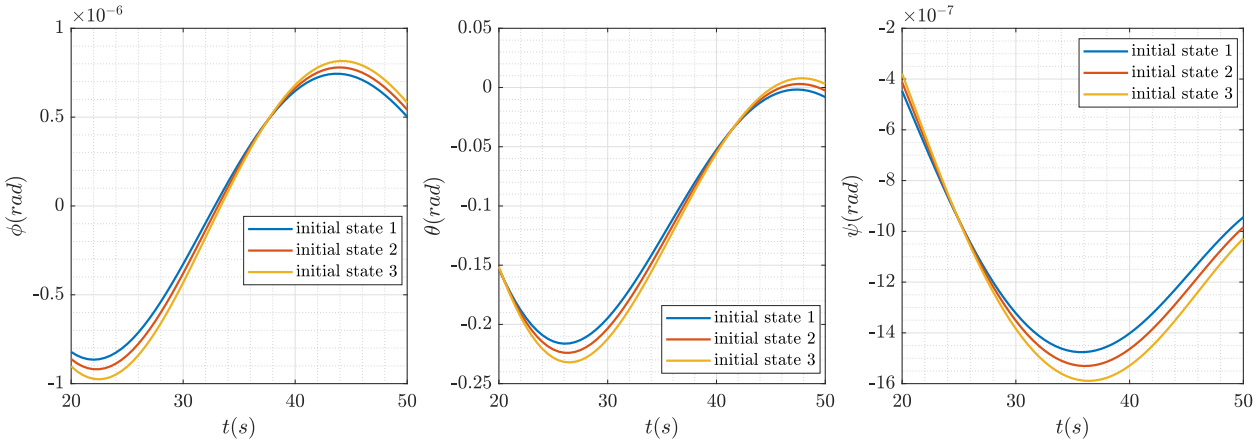

Figure 9: Regularity verification for kinematic equations

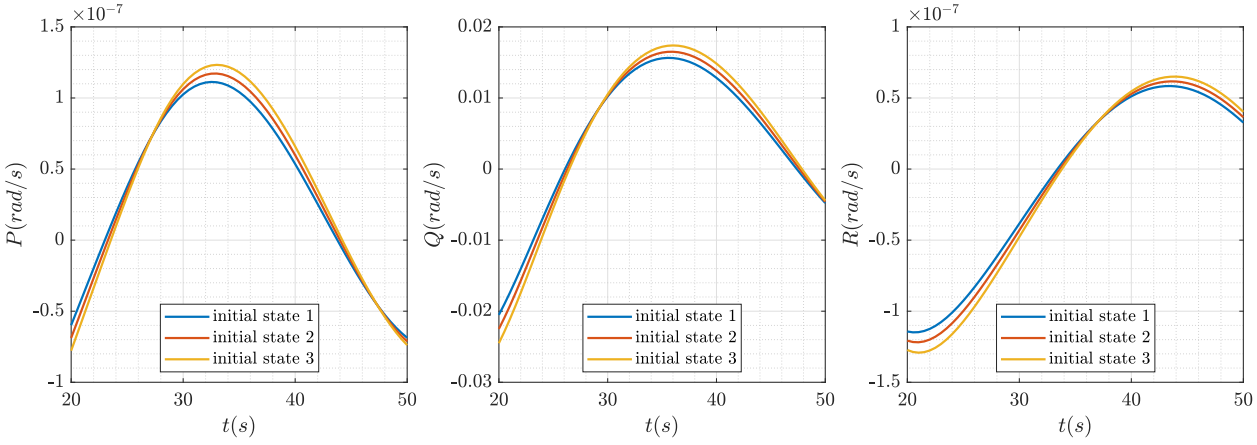

Figure 10: Regularity verification for moment equations

2.5 Invariance and Stability

An equilibrium point x^* of $\dot{x} = f(x)$, with $f : E \mapsto \mathbb{R}^n$ for $E \subset \mathbb{R}^n$ an open and connected set, is said to be stable if:

$$\forall \epsilon > 0, \quad \exists \delta > 0 \quad s.t. \quad \|x(t_0) - x^*\| < \delta \Longrightarrow \|x(t) - x^*\| < \epsilon, \quad \forall t \geq t_0 \tag{24}$$

Hence, Eq. 24 can be used to determine if the dynamical system is stable. For the dynamical system described in Sec. 2.1, the equilibrium point can be defined in Eq. 25. Since the dynamical system is composed of multiple equations, it is best to define a bound ϵ individually, as shown in Tab. 3. The ϵ is defined such that it is slightly larger than the norm between $x(t)$ and x^*. Simulations and errors are presented in Fig. 11-13, suggesting that the equilibrium points of the dynamical system are stable.

$$x^* = [80.0000, 0.0000, 3.2235, 0.0000, -0.0844, 0.0000, 0.0000, 0.0000, 0.0000] \tag{25}$$

Table 3: Stability Calculation

	U	V	W
$\|x(t) - x^*\|$	1.1696	1.4887e-07	0.0477
ϵ	1.2	1.5e-07	0.05
	ϕ	θ	ψ
$\|x(t) - x^*\|$	1.7820e-08	0.0031	1.7303e-08
ϵ	1.8e-08	0.005	1.8e-08
	P	Q	R
$\|x(t) - x^*\|$	3.0643e-09	4.7734e-04	1.7994e-09
ϵ	3.2e-09	4.8e-04	1.9e-08

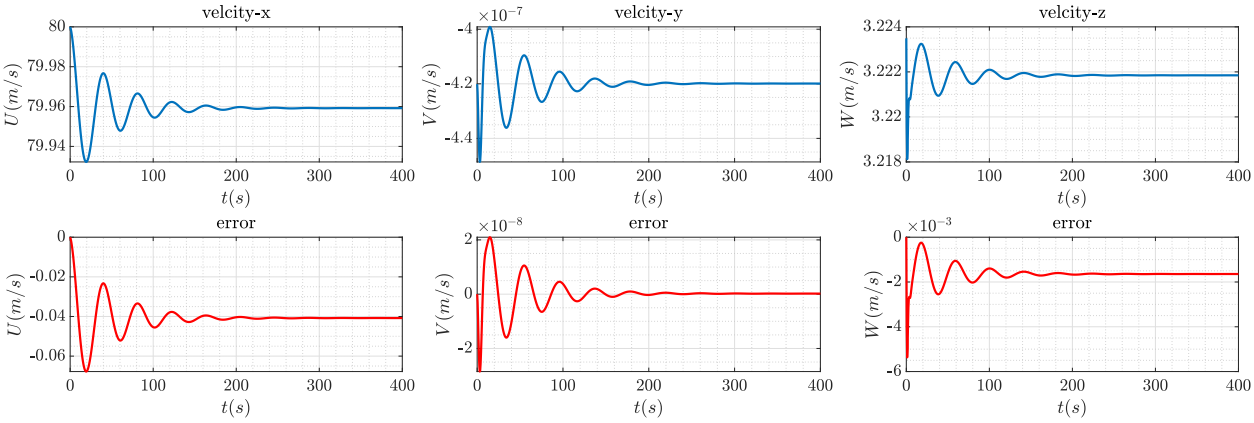

Figure 11: Stability verification for force equations

An invariant set can be defined as a set of points that is preserved under a given transformation or action. In other words, if the transformation is applied to any point in the

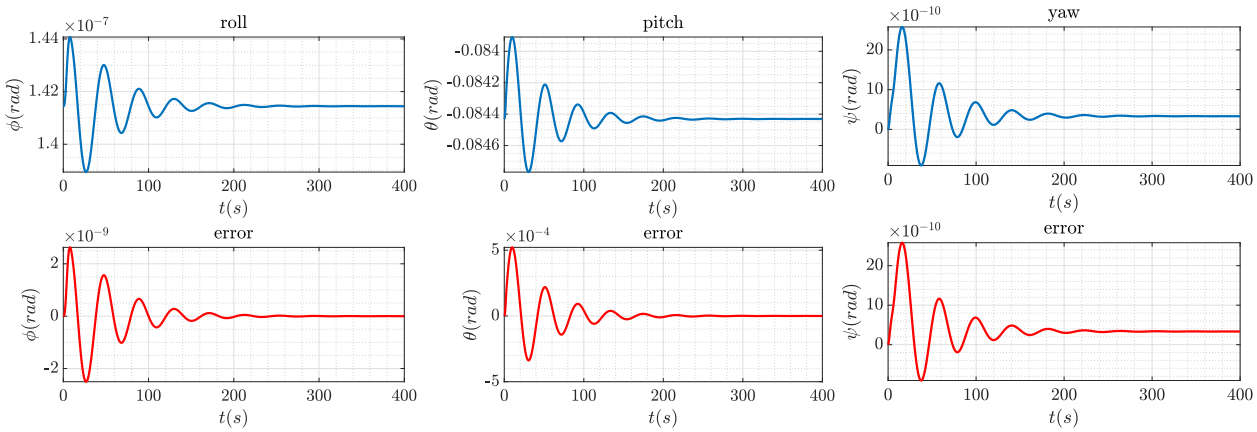

Figure 12: Stability verification for kinematic equations

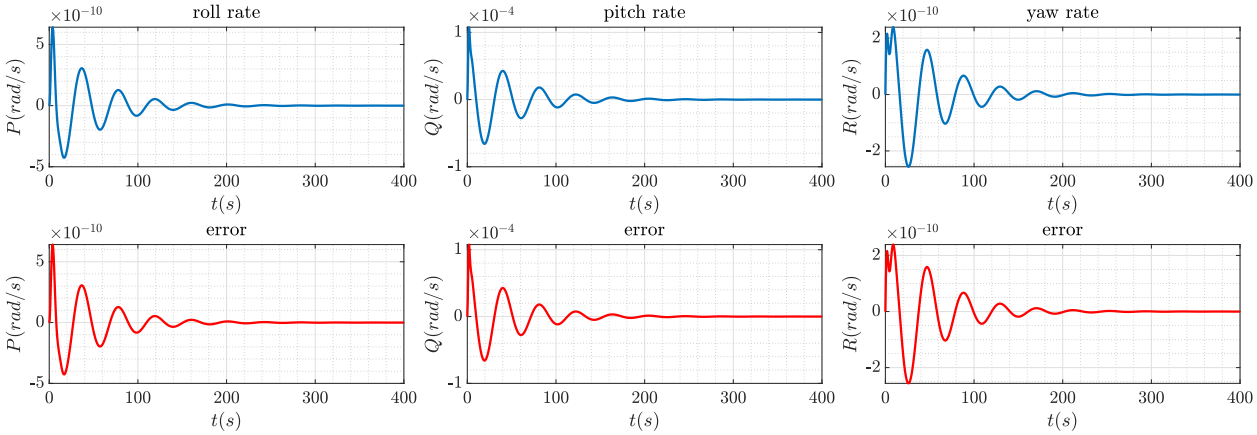

Figure 13: Stability verification for moment equations

invariant set, the resulting point is also in the set. Let $\Sigma = (T, X, \Phi, D_\Phi)$ be a dynamical system, where $T = [t_0, \infty]$ is a time-domain. Then, $A \subset X$ is called forward invariant if $x_0 \in A \Longrightarrow \Phi(t, x_0) \in A$ for all $t \in T_{\geq t_0}$. Additionally, a set of fixed points can be considered as an invariant set because these points remains unchanged under the transformation. Thus, invariant sets can be found by perturbing the system from the equilibrium points and observing the resulting behavior, as shown in Fig. 14-16. The resulting trajectories with perturbed initial conditions are converged to a certain region of the state space, suggesting these initial conditions are invariant sets of the system, as shown in Tab. 4.

Table 4: Invariant sets

	x_0
initial state 1	[82.00,0.0,3.22,0.0, -0.08,0.0,0.0,0.0,0.0,0.0]
initial state 2	[83.0,0.0,3.22,0.0, -0.08,0.0,0.0,0.0,0.0,0.0]
initial state 3	[84.0,0.0,3.22,0.0, -0.08,0.0,0.0,0.0,0.0,0.0]
initial state 4	[85.0,0.0,3.22,0.0, -0.08,0.0,0.0,0.0,0.0,0.0]

On the other hand, a limit point is defined as a point in the state space of a dynamical system that is approached by the trajectories of the system as time goes to infinity. As a result, a limit point in the dynamical system is a point that the system converges to asymptotically. Moreover, a limit point can be a fixed point, or a more complex invariant set. According to the simulation shown in Fig. 14-16, limit points can be identified by observing the long-term system behaviors. Since the solutions of the system converge to a constant value, which is a point that the trajectories of the system approach as time go to infinity, and therefore it is a limit point. The limit points are shown in Tab. 5.

Table 5: Limit points

	U	V	W
initial state 1	79.9591	-4.2015e-07	3.2218
initial state 2	79.9591	-4.2027e-07	3.2218
initial state 3	79.9591	-4.2039e-07	3.2218
initial state 4	79.9590	-4.2051e-07	3.2218
	ϕ	θ	ψ
initial state 1	1.4140e-07	-0.0844	3.9746e-09
initial state 2	1.4138e-07	-0.0844	1.3860e-10
initial state 3	1.4135e-07	-0.0844	-7.4831e-09
initial state 4	1.4133e-07	-0.0844	-1.8906e-08
	P	Q	R
initial state 1	2.3507e-12	-1.9310e-07	-4.5479e-12
initial state 2	3.5195e-12	-2.8632e-07	-6.7704e-12
initial state 3	4.6976e-12	-3.7884e-07	-8.9976e-12
initial state 4	5.8851e-12	-4.7070e-07	-1.1230e-11

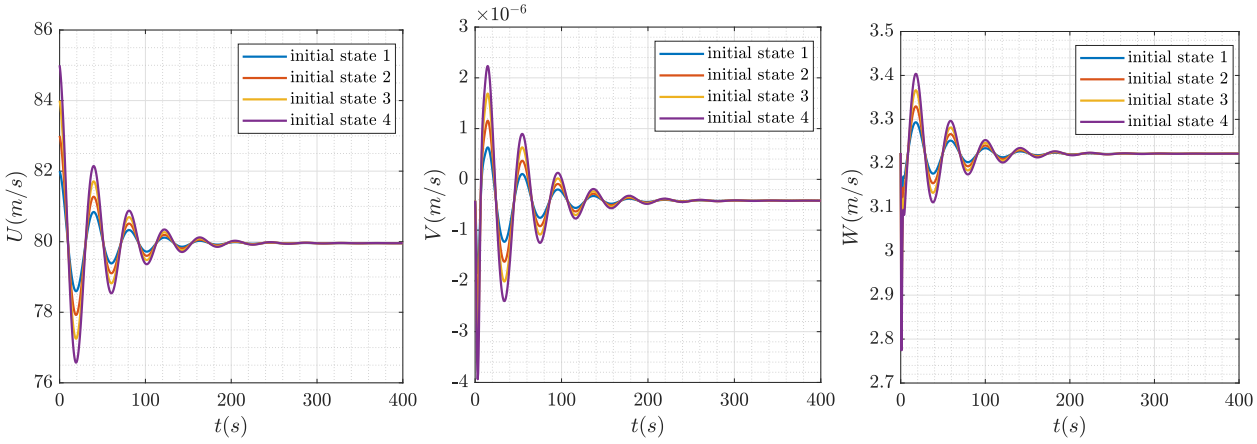

Figure 14: Invariant sets and limit points for force equations

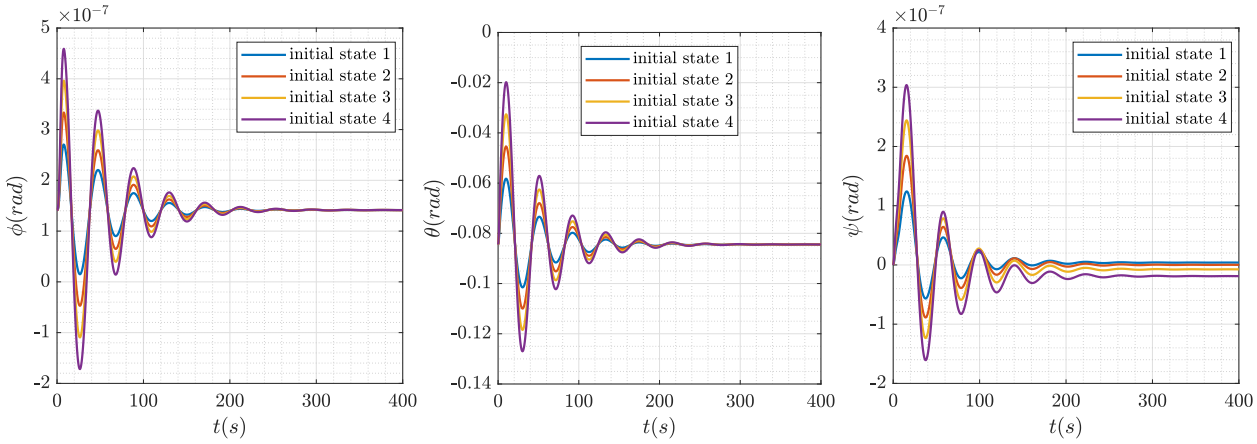

Figure 15: Invariant sets and limit points for kinematic equations

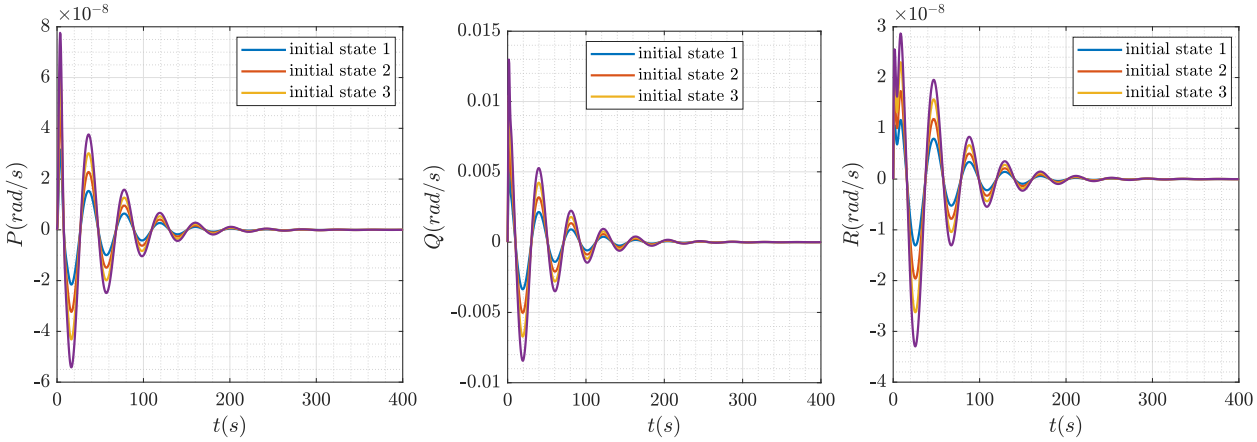

Figure 16: Invariant sets and limit points for moment equations

2.6 Lyapunov Method

Lyapunov method can be utilized to analyze the stability of the full-order dynamical system using a simpler representation of the system. Let $E \subseteq \mathbb{R}^n$ be an open and connected set containing the equilibrium point, $x^* = 0 \in E, x \mapsto x - x^*$, and let $V : E \mapsto \mathbb{R}$ be a continuously differentiable function. For a nonlinear system $\dot{x} = f(x)$, the derivative of Lyapunov function V along its solutions is given by:

$$\dot{V}(x) = \sum_{i=1}^{n} \frac{\partial V}{\partial x_i}\Big|_x \dot{x}_i = \sum_{i=1}^{n} \frac{\partial V}{\partial x_i}\Big|_x f_i(x) = \frac{\partial V}{\partial x}\Big|_x f(x) \tag{26}$$

Additionally, consider $\dot{x} = f(x)$ where $f : E \mapsto \mathbb{R}^n$ is a locally Lipschitz continuous function defined on the open and connected set $E \subseteq \mathbb{R}^n$. Let the equilibrium point $x^* = 0 \in E$ and the continuously differentiable function $V : E \mapsto \mathbb{R}$ satisfying $V(0) = 0$. Then, the equilibrium $x^* = 0$ is stable if:

- $V(x) > 0$ for all $x \in E \backslash \{0\}$

- $\dot{V}(x) \leq 0$ for all $x \in E$

Hence, a Lyapunov function for the system needs to be found. The scalar function $V(x)$ needs to be positive definite, ($V(0) = 0$ and $V(x) > 0$ for $x \neq 0$), and has a negative definite derivative along the trajectories of the system ($\dot{V}(x) < 0$ for $x \neq 0$). A good candidate for a Lyapunov function of aircraft dynamics is the energy of the system, which is a combination of the potential energy and kinetic energy, as shown in Eq. 29.

First, define the required components to formulate the Lyapunov function:

$$\begin{aligned} \dot{U} &= RV - QW - g\sin\theta + \frac{F_x}{m} \\ \dot{h} &= U\sin\theta - V\sin\phi\cos\theta - W\cos\phi\cos\theta \end{aligned} \tag{27}$$

Consider only linear motions of the aircraft in $\mathbb{R}^2$, Eq. 27 can be simplified as:

$$\begin{aligned} \dot{U} &= \frac{F_x}{m} \\ \dot{h} &= -W \end{aligned} \tag{28}$$

Express the Lyapunov function as a combination of the potential energy and kinetic energy:

$$\begin{aligned} V(x) &= \frac{1}{2}mv^2 + mgh \\ &= \frac{1}{2}mU^2 + mgh \\ &= \frac{1}{2}mx_1^2 + mgx_2 \end{aligned} \tag{29}$$

Equation 29 is clearly a positive definite function, where $V(x_1, x_2) \geq 0$ and $V(x_1, x_2) = 0$ if and only if $(x_1, x_2) = 0$. Now, let $x(t)$ be a solution to Eq. 28 with initial condition $x(t_0)$ at time t_0. Differentiating the Eq. 29 along these solution with respect to time yields:

$$\begin{aligned} \dot{V}(x) = \sum_{i=1}^{n} \frac{\partial V}{\partial x_i}\Big|_x \dot{x}_i &= \frac{\partial V}{\partial x_1}\Big|_{x(t)} \dot{x}_1(t) + \frac{\partial V}{\partial x_2}\Big|_{x(t)} \dot{x}_2(t) \\ &= mx_1\dot{x}_1 + mg\dot{x}_2 \\ &= mU\frac{F_x}{m} - mgW \\ &= UF_x - mgW \end{aligned} \tag{30}$$

Compute above equation at a equilibrium point, where $U = 0$ and $W = 0$:

$$\begin{aligned} \dot{V}(x) &= UF_x - mgW \\ &= 0 \end{aligned} \tag{31}$$

Therefore, $\dot{V} = 0$ and V is constant. Moreover, $V(x(t)) = V(x(t_0))$ and so solutions must stay in the set $V(x) \leq V(x(t_0))$ and thus the linear motion of the aircraft system is stable in $\mathbb{R}^2$.

3 Control Analysis

3.1 Control Inputs

Consider the dynamical system in Eq. 32-33, where $f(x,t)$ describes the aircraft's motion, including position, orientation, linear, and angular velocity. On the other hand, $g(x,t)$ is the control input of the system, representing the external forces and moments acting on the vehicle. Moreover, $g(x,t)$ can be controlled via input variables, such as aileron, rudder, elevator, and engine throttles. These input variables have a direct effect on the terms including:

- F_x: the force component acting in the x-direction
- F_y: the force component acting in the y-direction
- F_z: the force component acting in the z-direction
- $\bar{L}$: the moment about the x-axis (roll)
- M: the moment about the y-axis (pitch)
- Z: the moment about the z-axis (yaw)

It should be noted that all of these terms are in the body frame. Additionally, $f(x,t)$ and $g(x,t)$ are vector functions of states and time. Since the aircraft's motion, external forces, and moments evolve over time and states in response to various flight conditions.

$$\dot{x} = f(x,t) + g(x,t)u \tag{32}$$

$$\dot{x} = \begin{bmatrix} \dot{x_1} \\ \dot{x_2} \\ \dot{x_3} \\ \dot{x_4} \\ \dot{x_5} \\ \dot{x_6} \\ \dot{x_7} \\ \dot{x_8} \\ \dot{x_9} \end{bmatrix} = \begin{bmatrix} x_9x_2 - x_8x_3 - g_0' \sin x_5 \\ -x_9x_2 + x_7x_3 + g_0' \sin x_4 \cos x_5 \\ x_8x_1 - x_7x_2 + g_0' \cos x_4 \cos x_5 \\ x_7 + \tan x_5(x_8 \sin x_4 + x_9 \cos x_4) \\ x_8 \cos x_4 - x_9 \sin x_4 \\ \frac{x_8 \sin x_4}{\cos x_5} + \frac{x_9 \cos x_4}{\cos x_5} \\ (c_1x_9 + c_2x_7)x_8 \\ c_5x_7x_9 - c_6(x_7^2 - x_9^2) \\ (c_8x_7 - c_2x_9)x_8 \end{bmatrix} + \begin{bmatrix} \frac{F_x}{m} \\ \frac{F_y}{m} \\ \frac{F_z}{m} \\ 0 \\ 0 \\ 0 \\ c_3\bar{L} + c_4N \\ c_7M \\ c_4\bar{L} + c_9N \end{bmatrix} u \tag{33}$$

$$x = [U \quad V \quad W \quad \phi \quad \theta \quad \psi \quad P \quad Q \quad R]^T$$
$$u = [\delta_A \quad \delta_E \quad \delta_R \quad \delta_{TH_1} \quad \delta_{TH_2}]^T$$

3.2 Control Input Regularity

The control inputs described in Sec. 3.1 are expected to be continuous and differentiable at the equilibrium points because the dynamical system is assumed to be deterministic, in which

sensor noise, measurement errors, and actuator limitations do not exist. However, these stochastic effects appear in the real world and should be filtered and saturated to constrain the control inputs. Continuity is an essential property of control inputs since sudden changes or jumps in these signals can lead to unstable system behavior. For instance, abrupt changes in control surface positions can cause the aircraft to experience rapid changes in orientation, destabilizing the vehicle. Control inputs should also have differentiability, which can help to predict the system response.

Figure 17 presents the time-domain plots of control inputs, in which F_x, F_y, F_z, $\bar{L}$, M, and N are plotted as a function of time. By visual inspection, it can be easily observed that there are no sudden jumps or discontinuities in the signals. Therefore, the control inputs are continuous and differentiable. The first derivative of control inputs is plotted, as shown in the second row of Fig. 17. It can be concluded that the rate of change of some control inputs has a sudden peak at a certain point, indicating the function is not differentiable at that point. However, the behavior may be due to external disturbances in the system and may not indicate a sudden change in the system dynamics.

Moreover, the second derivative of control inputs is plotted, as shown in the third row of Fig. 17. The plots indicated that the control input has a peak, and the plot looks piece-wise continuous, suggesting that the control input is not twice differentiable. Thus, the system may have abrupt changes in the linear acceleration, velocity, and moments about the three axes, leading to system instability.

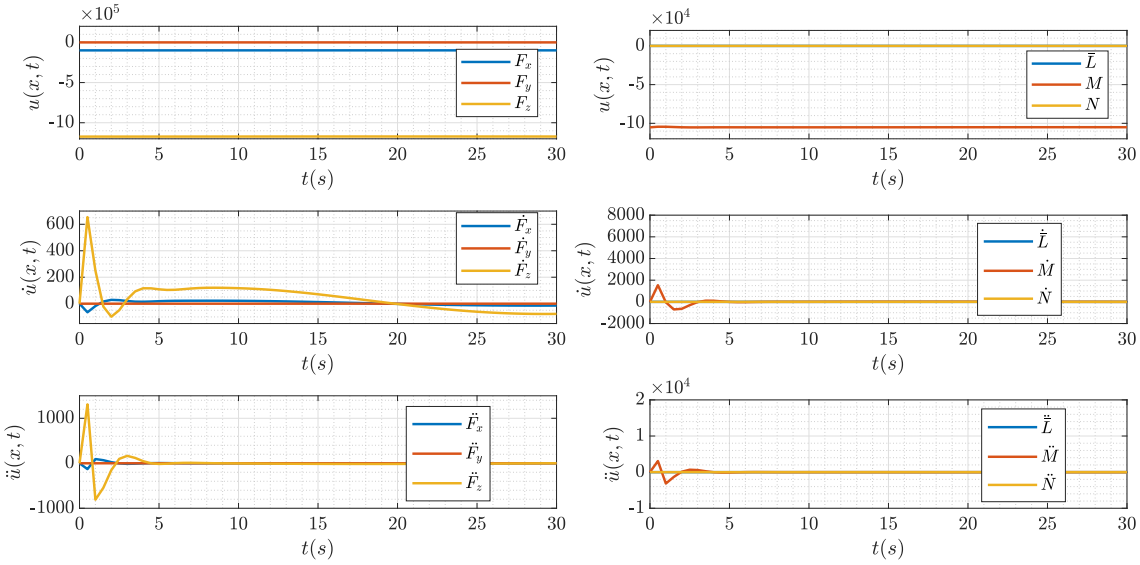

Figure 17: Control inputs

3.3 Output of Interest

Based on the state of the system, one possible output that can be regulated is the aircraft's altitude. Altitude control is an essential aspect of aircraft control design, in which the aircraft's altitude can be regulated by adjusting the control inputs such as engine throttle and control surface. In the dynamical system given in Sec. 3.1, the rate of change of altitude or the vertical velocity can be formulated in Eq. 47. According to the equation, the vertical

velocity is a function of three linear velocities U, V, W, and a function of two Euler angles ϕ, and θ. Therefore, regulating the altitude is equivalent to regulating the control input that maps to variables U, V, W, ϕ, and θ. The relationship is shown as follows:

- Aileron deflection: $\delta_A \mapsto \phi$
- Elevator deflection: $\delta_E \mapsto \theta$
- Engine throttles: $\delta_{TH_{1,2}} \mapsto U$
- V, W are coupled with U, ϕ, and θ
- Rudder deflection δ_R is not mapped because yaw angle ψ does not effect altitude

One way to achieve altitude control is to design a feedback controller that utilizes the vertical velocity error $e(s)$, such that the difference between the desired altitude $r(s)$ and the current altitude output $y(s)$ is minimized without destabilize the dynamical system.

$$\begin{aligned} \dot{h} &= U\sin\theta - V\sin\phi\cos\theta - W\cos\phi cos\theta \\ y &= h \end{aligned} \tag{34}$$

Figure 18 shows the altitude output of the system with control input $u = [\delta_A, \delta_E, \delta_R, \delta_{TH_1}, \delta_{TH_2}]^T = [0, -0.2196, 0, 0.0175, 0.0175]^T$.

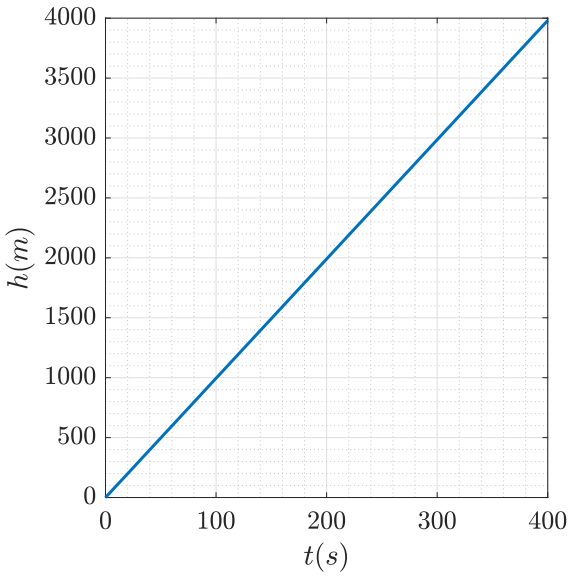

Figure 18: Altitude

3.4 Control Lyapunov Function

Finding the control Lyapunov function is often challenging because the function needs to satisfy the necessary conditions for stability and convergence. However, one common approach to finding the control Lyapunov function in the field is to linearize the dynamical system at the equilibrium points and solve for the linear Lyapunov function.

For aircraft dynamics, the system can be linearized under the following assumptions:

- the aircraft is rigid-body
- the aircraft's motion consists of small deviations from its equilibrium flight condition
- the motion of the aircraft can be analyzed by separating the equations into two groups (longitudinal and lateral motions)

Since the goal is to regulate the altitude of the aircraft, the linearization is concerned with the X-force, Z-force, and pitching moment equations, representing the longitudinal motion. The linearized dynamical system is shown in Eq. 35.

$$\begin{bmatrix} \Delta\dot{U} \\ \Delta\dot{W} \\ \Delta\dot{\theta} \\ \Delta\dot{Q} \end{bmatrix} = A \begin{bmatrix} \Delta U \\ \Delta W \\ \Delta\theta \\ \Delta Q \end{bmatrix} + B \begin{bmatrix} \delta_E \\ \delta_{TH_1} \\ \delta_{TH_2} \end{bmatrix} \tag{35}$$

$$\begin{bmatrix} \Delta\dot{x_1} \\ \Delta\dot{x_3} \\ \Delta\dot{x_5} \\ \Delta\dot{x_8} \end{bmatrix} = \begin{bmatrix} -0.03227 & 0.07526 & -9.775 & -3.118 \\ -0.2173 & -0.6715 & 0.8273 & 77.39 \\ 0 & 0 & 0 & 1 \\ 0.000941 & -0.03185 & 0 & -1.044 \end{bmatrix} \begin{bmatrix} \Delta x_1 \\ \Delta x_3 \\ \Delta x_5 \\ \Delta x_8 \end{bmatrix} + \begin{bmatrix} 0.2614 & 9.81 & 9.81 \\ -6.486 & 0 & 0 \\ 0 & 0 & 0 \\ -2.592 & 0.3924 & 0.3924 \end{bmatrix} \begin{bmatrix} \delta_E \\ \delta_{TH_1} \\ \delta_{TH_2} \end{bmatrix}$$

$$y = \begin{bmatrix} 0 & 0 & 0 & 0 \\ 0 & 0 & 0 & 1 \\ 0 & 0 & 0 & 0 \end{bmatrix} \begin{bmatrix} \Delta x_1 \\ \Delta x_3 \\ \Delta x_5 \\ \Delta x_8 \end{bmatrix}$$

The linear Lyapunov equation is given by:

$$AX + XA^T + Q = 0, \quad Q = C^T C \tag{36}$$

Solving Eq. 36, the solution to the Lyapunov equation can be calculated:

$$X = \begin{bmatrix} 2152.1 & -153.7 & -10.1 & 5.7 \\ -153.7 & 569.9 & 10.7 & 4.4 \\ -10.1 & 10.7 & 0.7 & 0.0 \\ 5.7 & 4.4 & 0.0 & 0.4 \end{bmatrix} \tag{37}$$

A candidate control Lyapunov function can be found using $V(x) = x^T X x$, where X is the solution to the linear Lyapunov equation, and x is the states in the dynamical system.

$$V(x) = \begin{bmatrix} x_1 & x_3 & x_5 & x_8 \end{bmatrix} \begin{bmatrix} 2152.1 & -153.7 & -10.1 & 5.7 \\ -153.7 & 569.9 & 10.7 & 4.4 \\ -10.1 & 10.7 & 0.7 & 0.0 \\ 5.7 & 4.4 & 0.0 & 0.4 \end{bmatrix} \begin{bmatrix} x_1 \\ x_3 \\ x_5 \\ x_8 \end{bmatrix} \tag{38}$$

$$V(x) = \begin{bmatrix} 2152.1x_1 - 153.7x_3 - 10.1x_5 + 5.7x_8 \\ -153.7x_1 + 569.9x_3 + 10.7x_5 + 4.4x_8 \\ -10.1x_1 + 10.7x_3 + 0.7x_5 \\ 5.7x_1 + 4.4x_3 + 0.4x_8 \end{bmatrix}^T \begin{bmatrix} x_1 \\ x_3 \\ x_5 \\ x_8 \end{bmatrix}$$

$$\begin{aligned} V(x) = x_1(2152.1x_1 - 153.7x_3 - 10.1x_5 + 5.7x_8) + x_3(-153.7x_1 + 569.9x_3 + 10.7x_5 + 4.4x_8) \\ +x_5(-10.1x_1 + 10.7x_3 + 0.7x_5) + x_8(5.7x_1 + 4.4x_3 + 0.4x_8) \end{aligned}$$

$$\begin{aligned} V(x) = 2152.1x_1^2 - 307.4x_1x_3 - 20.2x_1x_5 + 11.4x_1x_8 \\ +569.9x_3^2 + 21.4x_3x_5 + 5.5x_3x_8 + 0.7x_5^2 + 0.4x_8^2 \end{aligned}$$

The derivative of control Lyapunov functions is defined as $V : E \mapsto \mathbb{R}$, where its time derivative is expressed using Lie derivatives:

$$\dot{V}(x,u) = \frac{\partial V}{\partial x}\Big|_x f(x) + \frac{\partial V}{\partial x}\Big|_x g(x)u \triangleq L_f V(x) + L_g V(x)u \tag{39}$$

with $L_f V(x) \in \mathbb{R}$ and $L_g V(x) \in \mathbb{R}^{1\times m}$.

Additionally, for the nonlinear system, a control Lyapunov function (CLF) is a function $V : E \subseteq \mathbb{R}^n \mapsto \mathbb{R}$ satisfying the following conditions:

$$\lambda_1\|x\|^2 \leq V(x) \leq \lambda_2\|x\|^2, \quad \inf_{u\in U}[L_f V(x) + L_g V(x)u] \leq -\lambda_3 V(x) \tag{40}$$

for all $x \in E$ and positive constants λ_1,λ_2,$\lambda_3 \in \mathbb{R}_{>0}$.

Since regulating the aircraft's altitude involves controlling its vertical velocity or x_3, it is reasonable to take the derivative of the candidate control Lyapunov function along x_3. Moreover, the vertical velocity equation in the nonlinear system is given by:

$$\begin{aligned} \dot{x_3} &= x_8x_1 - x_7x_2 + g_0' \cos x_4 \cos x_5 + \frac{F_z}{m}u \\ f(x) &= x_8x_1 - x_7x_2 + g_0' \cos x_4 \cos x_5 \\ g(x)u &= \frac{F_z}{m}u \\ x &= [80.0, 0.0, 3.2235, 0.0, -0.0844, 0.0, 0.0, 0.0, 0.0]^T \end{aligned} \tag{41}$$

The derivative of control Lyapunov functions can be computed as:

$$\begin{aligned} \dot{V}(x,u) &= \frac{\partial V}{\partial x}\Big|_{x_3} f(x) + \frac{\partial V}{\partial x}\Big|_{x_3} g(x)u \\ &= (-307.4x_1 + 1139.8x_3 + 21.4x_5 + 5.5x_8)(x_8x_1 - x_7x_2 + g_0' \cos x_4 \cos x_5 + \frac{F_z}{m}u) \end{aligned}$$

Now, check if the candidate Lyapunov function satisfies the conditions in Eq. 40.

$$\begin{aligned} \lambda_1 6.4104e+03 \leq 1.3700e+07 \leq \lambda_2 6.4104e+03 \\ \inf_{u\in U}[-1.3651e+05] \leq -\lambda_3 6.4104e+03 \end{aligned} \tag{42}$$

Equation 42 indicated that the candidate CLF or $V(x)$ satisfies the CLF conditions, such that $\lambda_1\|x\|^2 \leq V(x) \leq \lambda_2\|x\|^2$, and $\inf_{u\in U}[L_fV(x) + L_gV(x)u] \leq -\lambda_3 V(x)$. Since $V(x)$ is bounded, in which three positive constants λ_1,λ_2,$\lambda_3 \in \mathbb{R}_{>0}$ can be defined. Therefore, $V(x)$ is a CLF for the aircraft dynamical system.

3.5 Input-to-State Stability

Input-to-state stability, or ISS, addresses the relationship between uncertainty and stability of control inputs to the dynamical system. Consider the system $\dot{x} = f(x, u)$, where $f : E \times \mathbb{R}^m \mapsto \mathbb{R}^n$ is a locally Lipschitz continuous function and $E \subseteq \mathbb{R}^n$ is an open and connected set for which $E \times \mathbb{R}^m$ contains the equilibrium pair $(x^*, u^*) = (0, 0)$, is Input-to-State Stable if there exist functions $\beta \in \mathcal{KL}$, $\gamma \in \mathcal{K}$, and $a \in \mathbb{R}_{>0}$ such that for every $t \leq t_0 = 0$ and every essentially bounded $u : \mathbb{R}_{\leq 0} \mapsto \mathbb{R}^m$. The definition is defined as:

$$\|x(t_0)\| \leq a \quad \Longrightarrow \quad \|x(t)\| \leq \beta(\|x(t_0)\|, t - t_0) + \gamma(\|u\|_\infty) \tag{43}$$

In other words, ISS guarantees that a small perturbation in the control input does not lead to a significant deviation in the output states. In general, proving ISS property involves finding a suitable ISS Lyapunov function and establishing the existence of functions $\beta \in \mathcal{KL}$ and $\gamma \in \mathcal{K}$, as well as a constant $a > 0$, such that the inequality in Eq. 43 holds. Nonetheless, finding an ISS Lyapunov function, or finding the β and γ functions are very challenging. Therefore, a weaker condition of Eq. 43 is utilized to prove the ISS property of the system, such that $\|x(t_0)\| \leq a$. Where a is a positive constant representing the initial condition bound, and it is chosen to be a design parameter.

To demonstrate the ISS stability of the system, Tab. 6 presents the numerical calculations of $\|x(t_0)\|$. Where u is selected to be essentially bounded based on the definition of ISS, and a is selected to satisfy the inequality of Eq. 43. Furthermore, the value of a determines the size of the ball around the equilibrium point (x^*, u^*). Within the ball, the system is stable for all essentially bounded inputs. Larger values of a provide a larger region of stability, and small values of a have a smaller region of stability. Based on the numerical calculations shown in Tab. 6, it can be observed that the aircraft dynamical system is ISS, such that $\|x(t_0)\| \leq a$.

Table 6: ISS verification

	U	V	W
$\|x(t_0)\|$	624.4740	3.2572e-06	25.1656
$\|u(t_0)\|$	7.7444e+05	1.2950	9.1516e+06
a	625	1.0	26
	ϕ	θ	ψ
$\|x(t_0)\|$	1.1048e-06	0.6582	1.3109e-08
$\|u(t_0)\|$	0	0	0
a	1.0	1.0	1.0
	P	Q	R
$\|x(t_0)\|$	2.4797e-09	4.0424e-04	1.4530e-09
$\|u(t_0)\|$	0.0038	8.2071e+05	24.4307
a	1.0	1.0	1.0

4 Control Law Design

4.1 Description of States, Outputs, and Controls of the System

Recall that the nonlinear aircraft dynamical system can be written in the form of affine control system, which is given by:

$$\dot{x}(x,t) = f(x,t) + g(x,t)u \tag{44}$$

$$\dot{x} = \begin{bmatrix} \dot{x_1} \\ \dot{x_2} \\ \dot{x_3} \\ \dot{x_4} \\ \dot{x_5} \\ \dot{x_6} \\ \dot{x_7} \\ \dot{x_8} \\ \dot{x_9} \end{bmatrix} = \begin{bmatrix} x_9x_2 - x_8x_3 - g_0' \sin x_5 \\ -x_9x_2 + x_7x_3 + g_0' \sin x_4 \cos x_5 \\ x_8x_1 - x_7x_2 + g_0' \cos x_4 \cos x_5 \\ x_7 + \tan x_5(x_8 \sin x_4 + x_9 \cos x_4) \\ x_8 \cos x_4 - x_9 \sin x_4 \\ \frac{x_8 \sin x_4}{\cos x_5} + \frac{x_9 \cos x_4}{\cos x_5} \\ (c_1x_9 + c_2x_7)x_8 \\ c_5x_7x_9 - c_6(x_7^2 - x_9^2) \\ (c_8x_7 - c_2x_9)x_8 \end{bmatrix} + \begin{bmatrix} \frac{F_x}{m} \\ \frac{F_y}{m} \\ \frac{F_z}{m} \\ 0 \\ 0 \\ 0 \\ c_3\bar{L} + c_4N \\ c_7M \\ c_4\bar{L} + c_9N \end{bmatrix} u \tag{45}$$

The states of the system is given by:

$$x = [U \quad V \quad W \quad \phi \quad \theta \quad \psi \quad P \quad Q \quad R]^T \tag{46}$$

Where the physical meaning of the states are associated with the motion and orientation of the aircraft. Each state is a vector function of time and it is defined to have the same dimension as the time vector t.

- $U \in \mathbb{R}^n, t \in \mathbb{R}^n$: linear velocity in x-axis
- $V \in \mathbb{R}^n, t \in \mathbb{R}^n$: linear velocity in y-axis
- $W \in \mathbb{R}^n, t \in \mathbb{R}^n$: linear velocity in z-axis
- $\phi \in \mathbb{R}^n, t \in \mathbb{R}^n$: roll angle
- $\theta \in \mathbb{R}^n, t \in \mathbb{R}^n$: pitch angle
- $\psi \in \mathbb{R}^n, t \in \mathbb{R}^n$: yaw angle
- $P \in \mathbb{R}^n, t \in \mathbb{R}^n$: roll rate
- $Q \in \mathbb{R}^n, t \in \mathbb{R}^n$: pitch rate
- $R \in \mathbb{R}^n, t \in \mathbb{R}^n$: yaw rate

One potential output of the system is the altitude measurement h, which is coupled with other states including U, V, θ, and ϕ. The measurement is a vector function and it has the same dimension as time t, such that $y \in \mathbb{R}^n, t \in \mathbb{R}^n$.

$$\begin{aligned} \dot{h} &= U \sin\theta - V \sin\phi \cos\theta - W \cos\phi cos\theta \\ \dot{y} &= \dot{h} \\ y &= h \end{aligned} \tag{47}$$

The perturbation of the system is described by

$$g(x,t) = [\frac{F_x}{m} \quad \frac{F_y}{m} \quad \frac{F_z}{m} \quad 0 \quad 0 \quad 0 \quad c_3\bar{L} + c_4 N \quad c_7 M \quad c_4\bar{L} + c_9 N]^T \tag{48}$$

The physical meaning of each perturbation component is defined as:

- $F_x \in \mathbb{R}^n, t \in \mathbb{R}^n$: the force component acting in the x-direction
- $F_y \in \mathbb{R}^n, t \in \mathbb{R}^n$: the force component acting in the y-direction
- $F_z \in \mathbb{R}^n, t \in \mathbb{R}^n$: the force component acting in the z-direction
- $\bar{L} \in \mathbb{R}^n, t \in \mathbb{R}^n$: the moment about the x-axis (roll)
- $M \in \mathbb{R}^n, t \in \mathbb{R}^n$: the moment about the y-axis (pitch)
- $Z \in \mathbb{R}^n, t \in \mathbb{R}^n$: the moment about the z-axis (yaw)
- $c_i \in \mathbb{R}^n, t \in \mathbb{R}^n$: fixed constants depend on the geometry of the rigid-body aircraft

The perturbation $g(x,t)$ is directed by the control input u, which is given by

$$u = [\delta_A \quad \delta_E \quad \delta_R \quad \delta_{TH_1} \quad \delta_{TH_2}]^T \tag{49}$$

The physical meaning of each control input component is defined as:

- $\delta_A \in \mathbb{R}^n, t \in \mathbb{R}^n$: aileron deflection
- $\delta_E \in \mathbb{R}^n, t \in \mathbb{R}^n$: elevator deflection
- $\delta_{TH_{1,2}} \in \mathbb{R}^n, t \in \mathbb{R}^n$: engine throttle positions
- $\delta_R \in \mathbb{R}^n, t \in \mathbb{R}^n$: rudder deflection

At each time step, there is a control input saturation to keep the dynamical system well defined for all time. The saturation limits are a reasonable assumption, because real physical actuators have similar constraints.

- $\delta_A \in [-25°, 25°], \forall t$
- $\delta_E \in [-25°, 10°], \forall t$
- $\delta_{TH_{1,2}} \in [\frac{0.5\pi}{180}, \frac{\pi}{180}], \forall t$
- $\delta_R \in [-30°, 30°], \forall t$

4.2 Feedback Linearization

Feedback linearization is a powerful technique used in nonlinear control problems. Such technique can be used to exactly linearize a part of a nonlinear system via a nonlinear controller for a specific class of systems. To begin feedback linearization process, the definition of affine control systems and control objectives need to be introduced.

4.2.1 Theory

Let $E \subseteq \mathbb{R}^n$ be an open and connected set and consider a set of admissible control inputs $U \subseteq \mathbb{R}^m$. A control system is an affine control system (or control affine) if it can be written in the form:

$$\dot{x} = f(x,t) + g(x,t)u \tag{50}$$

with $x \in E, u \in U$, and where:

$$f : E \mapsto \mathbb{R}^n, \quad g : E \mapsto \mathbb{R}^{n \times m}$$

are continuously differentiable functions. The term f is called the drift and the term g is called the actuation matrix, the control matrix, or the input matrix. Moreover, an output for the system in Eq. 50 can be represented by a differentiable function $h : E \subseteq \mathbb{R}^n \mapsto \mathbb{R}^k$, and written as a vector of k function:

$$y \triangleq h(x,t) = [h_i(x,t)]_{i=,1,\ldots,k} = \begin{bmatrix} h_1(x,t) \\ h_2(x,t) \\ \cdot \\ \cdot \\ \cdot \\ h_k(x,t) \end{bmatrix} \in \mathbb{R}^k \tag{51}$$

The goal of feedback linearization is to find a feedback control law $u = k(x,t), k : E \subset \mathbb{R}^m \mapsto U$, such that any solution $x(t)$ of the resulting closed-loop system:

$$\dot{x} = f_{cl}(x,t) = f(x,t) + g(x,t)k(x,t) \tag{52}$$

satisfies the control objective:

$$y(x,t) = h(x,t) \to 0, \quad t \to \infty$$

One standard control objective is to drive the system to a desired state $x_{des} \in \mathbb{R}^n$ and the output can be formulated as:

$$h(x,t) = x(t) - x_{des}(t)$$

where $h : E \to \mathbb{R}^n$ and thus $k = n$.

4.2.2 Feedback Linearizable

As mentioned earlier, the feedback linearization approach may not apply to all class of nonlinear dynamical systems, and thus the notion of feedback linearizable needs to be introduced and verified for the aircraft system.

An affine control system is feedback linearizable if there exist a feedback control law $u = k(x, v), k : E \times V \to U$ for $V \subset \mathbb{R}$, and $\gamma \in \{1, ..., n\}$ such that:

$$\dot{x} = f(x) + g(x)k(x, v) \quad \Longrightarrow \quad y^{(\gamma)} \triangleq h^{(\gamma)}(x) = v \tag{53}$$

for a new control input or an auxiliary input $v \in V \subset \mathbb{R}$. The notation $y^{(\gamma)}$ denotes the γ^{th} time derivative of y along solutions. The linear relationship $y^{(\gamma)} = v$ indicated that v can be used to shape the evolution of the output $y = h(x)$ and its time derivative.

Consider a minimum realization (**longitudinal motion only**) of the nonlinear aircraft model without loss of generality:

$$\dot{x} = \begin{bmatrix} \dot{x_1} \\ \dot{x_3} \\ \dot{x_5} \\ \dot{x_8} \end{bmatrix} = \begin{bmatrix} -x_8 x_3 - g_0' \sin x_5 \\ x_8 x_1 + g_0' \cos x_5 \\ x_8 \\ -c_6 x_7^2 \end{bmatrix} + \begin{bmatrix} \frac{F_x}{m} \\ \frac{F_z}{m} \\ 0 \\ 0 \end{bmatrix} u \tag{54}$$

The states of the system is given by:

$$x = [U \quad W \quad \theta \quad Q]^T \tag{55}$$

The output of the system is given by:

$$\dot{y}(x) \triangleq \dot{h}(x) = x_1 \sin x_5 - x_3 \cos x_5 \tag{56}$$

The control objective is to drive $y(x) = h(x) \to 0, \quad t \to \infty$. Therefore, a candidate controller with the assumption of $\gamma = 1$ can be considered as:

$$\begin{aligned} v &= -\alpha y \\ v &= -\alpha(x_1 \sin x_5 - x_3 \cos x_5) \\ v &= -\alpha x_1 \sin x_5 + \alpha x_3 \cos x_5 \end{aligned} \tag{57}$$

Therefore, feedback linearization is applicable to the longitudinal nonlinear aircraft model since the system satisfy the requirement of $y^{(\gamma)} \triangleq h^{(\gamma)}(x) = v$. The feedback linearization may be also applied to the full-order nonlinear aircraft model, but the linear relationship is difficult to identify.

4.2.3 Relative Degree

A key concept of feedback linearization is the notion of relative degree γ, where $\gamma \in \mathbb{N}$ is the smallest positive integer satisfying:

$$\forall x \in E, \quad \forall i = 0, ..., \gamma - 2, \quad L_g L_f^i h(x) = 0, \iff \gamma \geq 2 \tag{58}$$

then the output $y = h(x)$ has relative degree of γ and it can be written as:

$$y^{(\gamma)} = L_f^\gamma h(x) + L_g L_f^{\gamma-1} h(x) u \tag{59}$$

Thus, the control law:

$$u = k(x, v) = \frac{1}{L_g L_f^{\gamma-1} h(x)} (-L_f^\gamma h(x) + v) \tag{60}$$

leads to a linear relationship between the input and the output:

$$y^{(\gamma)} = v \tag{61}$$

Consider the minimum realization of the plant in Sec. 4.2.2, where $f(x)$, $h(x)$ and $g(x)$ are given by:

$$f(x) = \begin{bmatrix} -x_8 x_3 - g_0' \sin x_5 \\ x_8 x_1 + g_0' \cos x_5 \\ x_8 \\ -c_6 x_7^2 \end{bmatrix}, \quad g(x) = \begin{bmatrix} \frac{F_x}{m} \\ \frac{F_z}{m} \\ 0 \\ 0 \end{bmatrix}, \quad h(x) = x_1 \sin x_5 - x_3 \cos x_5 \tag{62}$$

differentiating the output yields:

$$\frac{\partial h}{\partial x}\Big|_{x_1, x_3, x_5, x_8} = \begin{bmatrix} \sin x_5 & -\cos x_5 & x_1 \cos x_5 & 0 \end{bmatrix} \tag{63}$$

$$\begin{aligned} L_f h(x) &= \frac{\partial h}{\partial x}\Big|_{x_1, x_3, x_5, x_8} f(x) \\ &= \begin{bmatrix} \sin x_5 & -\cos x_5 & x_1 \cos x_5 & 0 \end{bmatrix} \begin{bmatrix} -x_8 x_3 - g_0' \sin x_5 \\ x_8 x_1 + g_0' \cos x_5 \\ x_8 \\ -c_6 x_7^2 \end{bmatrix} \\ &= \sin x_5 (-x_8 x_3 - g_0' \sin x_5) - \cos x_5 (x_8 x_1 + g_0' \cos x_5) + (x_1 \cos x_5) x_8 \end{aligned} \tag{64}$$

$$\begin{aligned} L_g h(x) &= \frac{\partial h}{\partial x}\Big|_{x_1, x_3, x_5, x_8} g(x) \\ &= \begin{bmatrix} \sin x_5 & -\cos x_5 & x_1 \cos x_5 & 0 \end{bmatrix} \begin{bmatrix} \frac{F_x}{m} \\ \frac{F_z}{m} \\ 0 \\ 0 \end{bmatrix} \\ &= \sin x_5 (\frac{F_x}{m}) - \cos x_5 (\frac{F_z}{m}) \end{aligned} \tag{65}$$

$$
\begin{aligned}
L_g L_f h(x) &= \left.\frac{\partial L_f h}{\partial x}\right|_{x_1,x_3,x_5,x_8} g(x) \\
&= \begin{bmatrix} x_8 \cos x_5 & -x_8 \sin x_5 & * & * \end{bmatrix} \begin{bmatrix} \frac{F_x}{m} \\ \frac{F_z}{m} \\ 0 \\ 0 \end{bmatrix} \\
&= x_8 \cos x_5 \frac{F_x}{m} - x_8 \sin x_5 \frac{F_z}{m} \neq 0
\end{aligned} \tag{66}
$$

Since $L_g L_f h(x) \neq 0, \quad \forall x$, it can be concluded that the system has a relative degree of 1.

4.2.4 Zero-Dynamics

Section 4.2.3 suggested that the minimum realization of the nonlinear aircraft system has a relative degree of 1 for a system of dimension 4. As a result, the system has zero dynamics because the relative degree is smaller than the system dimension. Zero-dynamics behavior indicated that some modes in the system are not observable from the output measurement or controllable by the control inputs. The impulse response of the output is simulated to check if the zero-dynamics behavior is stable, as shown in Fig. 19. Based on the simulation results, the zero-dynamics is stable as t approach ∞.

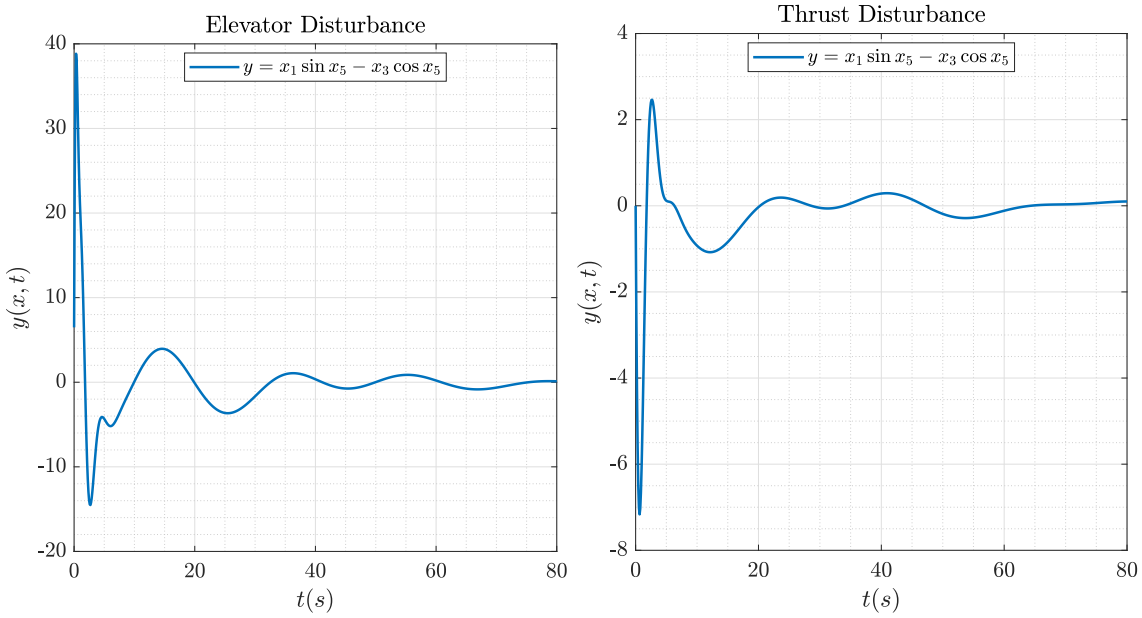

Figure 19: Impulse response of the output

4.3 Back-Stepping Lyapunov Function

While feedback linearization is a powerful tool for nonlinear control, the approach heavily depends on the accuracy of the system model. To have a more robust controller and model

uncertainty, back-stepping method is commonly used to stabilize nonlinear systems using Lyapunov functions to recursively design a feedback control law that stabilizes the system. The challenging part of back-stepping method is that it requires the nonlinear system with a special structure called strict feedback form:

$$\begin{aligned}
\dot{x} &= f_0(x) + g_0(x)z_1 \\
\dot{z}_1 &= f_1(x, z_1) + g_1(x, z_1)z_2 \\
\dot{z}_2 &= f_2(x, z_1, z_2) + g_2(x, z_1, z_2)z_3 \\
&\cdot \\
&\cdot \\
&\cdot \\
\dot{z}_k &= f_k(x, z_1, z_2, ..., z_k) + g_k(x, z_1, z_2, ..., z_k)u
\end{aligned} \tag{67}$$

where $x \in E \subseteq \mathbb{R}^n$, virtual controllers $z_1, ..., z_k \in \mathbb{R}$, and $u \in \mathbb{R}$.

Consider the longitudinal motion of the nonlinear aircraft system:

$$\dot{x} = \begin{bmatrix} \dot{x}_1 \\ \dot{x}_3 \\ \dot{x}_5 \\ \dot{x}_8 \end{bmatrix} = \begin{bmatrix} -x_8 x_3 - g_0' \sin x_5 \\ x_8 x_1 + g_0' \cos x_5 \\ x_8 \\ -c_6 x_7^2 \end{bmatrix} + \begin{bmatrix} \frac{F_x}{m} \\ \frac{F_z}{m} \\ 0 \\ 0 \end{bmatrix} u \tag{68}$$

Introduce a variable called "true velocity" $\dot{V}_T$ to combine $\dot{x}_1$ and $\dot{x}_3$:

$$\dot{V}_T = \frac{x_1 \dot{x}_1 + x_3 \dot{x}_3}{V_T} \tag{69}$$

Express the above system in strict feedback form:

$$\begin{aligned}
\dot{V}_T &= \frac{x_1 \dot{x}_1 + x_3 \dot{x}_3}{V_T} \\
\dot{x}_5 &= x_8 \\
\dot{x}_8 &= u, \quad u = -c_6 x_7^2
\end{aligned} \tag{70}$$

Assume the control law $z_1 = kx$ renders the equilibrium $x^* = 0$ of Eq. 70 asymptotically stable and that the CLF $V_x : \mathbb{R}^n \mapsto \mathbb{R}_{\geq 0}$ is a corresponding Lyapunov function satisfying $\dot{V}_x(x) \leq -\alpha(||x||)$ for some κ function α. Then, the control law is given by:

$$u = \frac{1}{g_1(x, z_1)}(-f_1(x, z_1) - \frac{\partial V_x}{\partial x}\Big|_x g_0(x) - \sigma(z_1 - k(x)) + \frac{\partial k}{\partial x}\Big|_x (f_0(x) + g_0(x)z_1)) \tag{71}$$

As a result, a control law that stabilize the closed-loop system can be found by utilizing the above formula. Since the nonlinear aircraft system can be formulated into a strict feedback form, the recursive design for a Lyapunov function using back-stepping approach is applicable to the system.

5 Conclusion

References

[1] B. L. Stevens, F. L. Lewis, and E. N. Johnson, *Aircraft control and simulation: dynamics, controls design, and autonomous systems*. John Wiley & Sons, 2015.

[2] F. GARTEUR, "Robust flight control design challenge problem formulation and manual: the research civil aircraft model (rcam)," tech. rep., GARTEUR, 1995. URL http://www. garteur. org/Technical% 20Reports ....

[3] R. C. Nelson *et al.*, *Flight stability and automatic control*, vol. 2. WCB/McGraw Hill New York, 1998.